Models of natural stochastic textures and their applications in image processing

Thesis proposal

Ido Zachevsky

Under the supervision of Prof. Yehoshua Y. Zeevi

January 22, 2014

Outline

The structure of natural images (I)

- Blue – segments of natural images.
- "Classical" model.
- Properties?
- Enhacement?

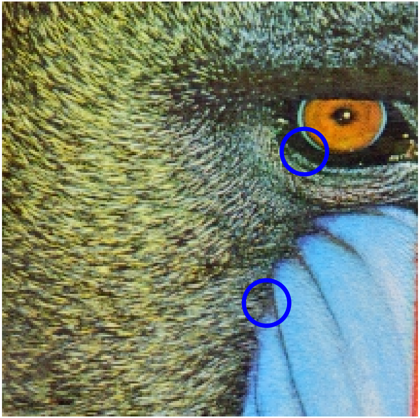

Original image

The structure of natural images (I)

- Blue – segments of natural images.
- "Classical" model.
- Properties? **Smooth surfaces separated by edges.**
- Enhacement? **Contour empasis, smoothing of low gradients.**

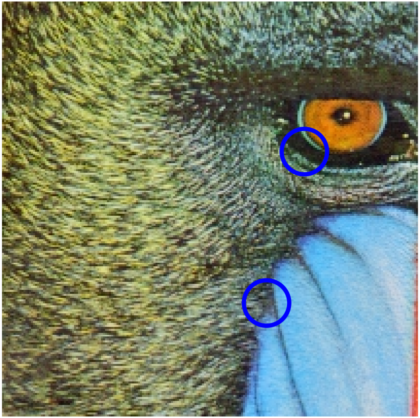

Original image

The structure of natural images (I)

- Blue – segments of natural images.
- "Classical" model.
- Properties? **Smooth surfaces separated by edges.**
- Enhacement? **Contour empasis, smoothing of low gradients.**

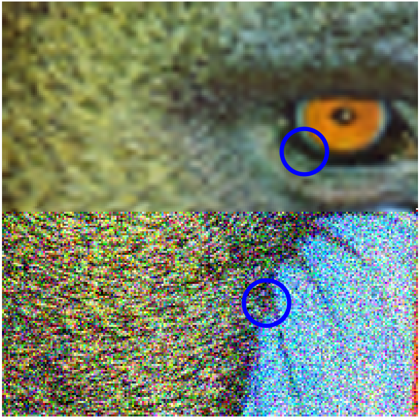

Noisy or low-resolution image

The structure of natural images (II)

- Red – segment of a natural stochastic texture.
- Does the classical model fit?
- Properties?
- Statistics?
- Enhacement?

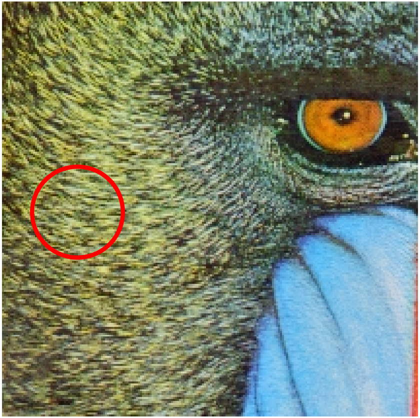

Original image

The structure of natural images (II)

- Red – segment of a natural stochastic texture.
- Does the classical model fit?
- Properties? **Low gradients and fine details not generated by edges.**
- Statistics? **Gaussian, self-similar**
- Enhacement? **The subject of this research.**

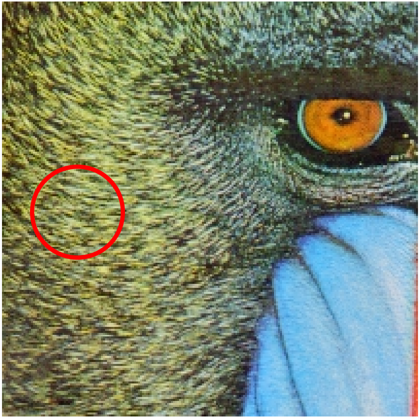

Original image

The structure of natural images (II)

- Red – segment of a natural stochastic texture.
- Does the classical model fit?
- Properties? **Low gradients and fine details not generated by edges.**
- Statistics? **Gaussian, self-similar**
- Enhacement? **The subject of this research.**

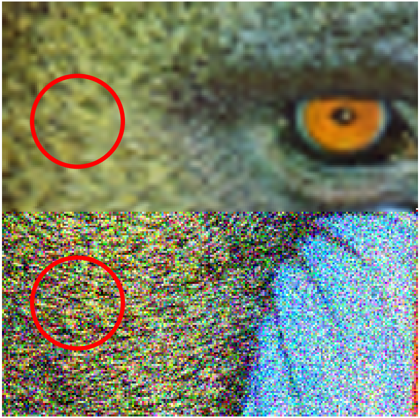

Noisy or low-resolution image

Natural stochastic textures (NST) in natural images

Natural stochastic textures are abundant in natural images.

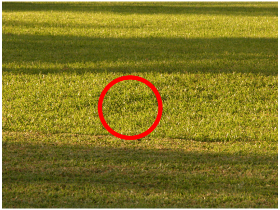
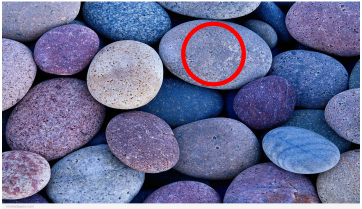
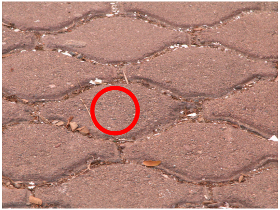


⋆ Current study performed on images with a single texture.

Outline

Statistics of natural images (I)

- Gaussian scale mixtures (GSM) [Portilla et al., 2003]

$$Y \overset{d}{=} \sqrt{Z}X, \quad X \sim \mathcal{N}(m, \Lambda), \quad P_Z(z) = z^{-1} \tag{1}$$

- Generalized Gaussian distributions [Srivastava et al., 2003]

$$f_X(x) = \frac{\beta}{2\alpha\Gamma(1/\beta)} e^{-(|x-\mu|/\alpha)^{\beta}}, \beta \in [0.5, 1] \tag{2}$$

- Markov random fields (MRF) in a low order, $G = (V, E)$ [Perez, 1998, Li, 2009].

$$P(X = x) = \frac{1}{Z(\beta)} e^{-\beta E(x)} \tag{3}$$

Statistics of natural images (II)

- Gaussian mixture models (GMM) [Zoran, 2012].

$$p(x;\theta) = \sum_{i=1}^{K} \pi_i \mathcal{N}(x;\mu_i,\Sigma_i) \tag{4}$$

- Field of Experts (FoE) model [Roth and Black, 2009]

$$f(x;\Theta) = \frac{1}{Z(\theta)} \prod_{k=1}^{K} \prod_{i=1}^{N} \phi(J_i^T x_k;\theta_i) \tag{5}$$

- Sparsity [Elad and Figueiredo, 2010]

$$x = D\alpha \tag{6}$$

Statistics of natural images (III)

Properties of existing natural image models:

- *Leptokurtic* distributions – choice of Experts, GSM, Generalized Gaussian with $\beta \leq 1$.
- Patch or otherwise *locally* based – GMM, MRF (clique size), sparsity.
- Learning distributions from samples – GMM, FoE, MRF, sparsity.

Main conclusion

Ensambles of natural images have *non-Gaussian* statistics.

Analysis method:

- Analyzing wavelet coefficients or other derivative filters.
- First and second order empirical distributions (histograms).

Statistics of *natural stochastic textures* (NST) (I)

Properties of NSTs include:

- *Gaussian* statistics in marginal and joint distributions, unlike general natural images. [Zachevsky and Zeevi, 2014]
  - In image space.
  - In wavelet domain.
- Self similarity – scale invariance [Srivastava et al., 2003].
- NSTs are considered as 2D realizations of random processes.

Main conclusion from current study

Natural stochastic textures have *Gaussian* statistics.

A suitable model should be *Gaussian and self-similar*.

Statistics of *natural stochastic textures* (NST) (II)

Wavelet domain statistics: Steerable pyramids

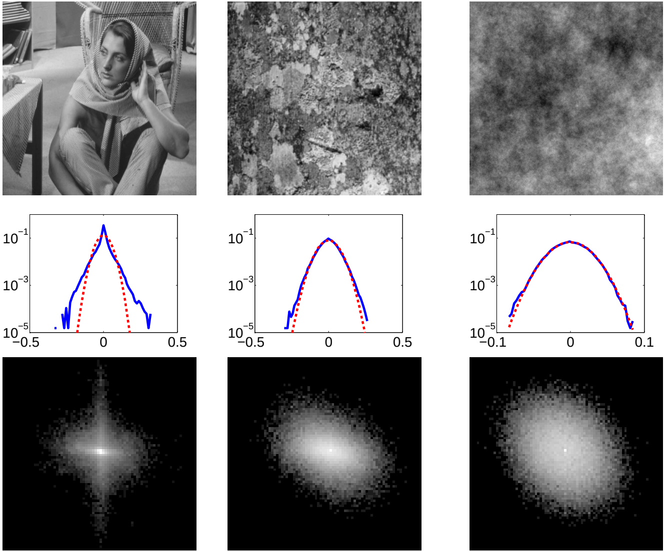

Natural image | Stochastic texture | Synthetic texture (fBm)

Statistics of *natural stochastic textures* (NST) (III)

Image domain statistics

Statistics of *natural stochastic textures* (NST) (III)

Image domain statistics

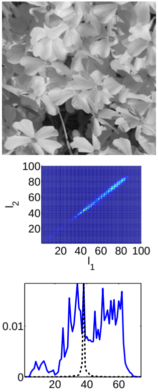

Natural image

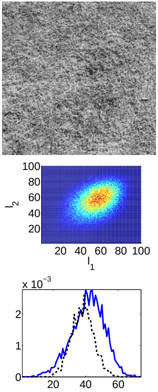

Stochastic texture (1)

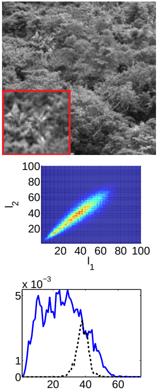

Stochastic texture (2)

Determining Gaussianity

Hypothesis testing

- Testing Gaussianity versus non-Gaussianity.
- H_0: NST, as a subset of images, are non-Gaussian.
- H_1: NST are Gaussian.
- Possible statistic: Excess kurtosis; $Kurt(X) = 0$ for Gaussian, $Kurt(X) > 0$ in leptokurtic distributions.
- More complex tests: Jarque-Bera test [Jarque and Bera, 1980, Gel and Gastwirth, 2008]

$$JB = \frac{n}{6}\left(\frac{\hat{\mu}_3}{\hat{\mu}_2^{3/2}}\right)^2 + \frac{n}{24}\left(\frac{\hat{\mu}_4}{\hat{\mu}_2} - 3\right)^2. \tag{7}$$

- For independent samples.

⋆ Normality testing is a known field of research.

Outline

NST models: Desired properties

- Gaussianity [Zachevsky and Zeevi, 2013a].
- Self-similarity in the statistical sense (fractal):

$$X(ct) \stackrel{d}{=} c^{\alpha} X(t), c > 0 \tag{8}$$

- Locality: NST exhibit long-range dependencies (*LRD*) [Samorodnitsky, 2005, Eom, 2001, Pesquet-Popescu and Vehel, 2002, Kashyap and Lapsa, 1984, Gilboa and Osher, 2008],

$$\sum_{n=0}^{\infty} r_n = \infty \tag{9}$$

Translation of these qualities to random processes properties:

- Self-similarity $\Rightarrow X(0) = 0 \Rightarrow$ Cannot be stationary.
- Long-range dependence: $r_n \propto n^{-d}$ where $0 < d < 1$ (can be stationary).

Example: AR(1) - an unsuitable model.

$$X(n+1) = aX(n) + N(n) \Rightarrow r_n = \frac{\sigma_N^2}{1-a^2} a^{|n|} \tag{10}$$

Fractional Brownian motion (fBm)

[Mandelbrot and Van Ness, 1968, Kolmogorov, 1940]

FBm $\Rightarrow$ Gaussianity and self-similarity [Samorodnitsky, 2005]:

1. $B(\{t_1, t_2, \ldots, t_k\}) \sim \mathcal{N}(0, \Sigma(\{t_i\}))$
2. $B(ct) \overset{d}{=} c^H B(t), c > 0$
3. Stationary increments.

$\Rightarrow B(t)$ is fBm with a self-similarity parameter $H \in (0, 1)$ and autocorrelation:

$$E\left[B_H(t)B_H(s)\right] = \frac{\sigma_H^2}{2}\left(|t|^{2H} + |s|^{2H} - |t-s|^{2H}\right)$$

Properties with respect to H:

- $0 < H < \frac{1}{2}$: Short-range dependence and antipersistence (high frequencies).
- $H = \frac{1}{2}$: Brownian motion, $E[B_H(t)B_H(s)] \propto s \wedge t$.
- $\frac{1}{2} < H < 1$: Long-range dependence and persistence (low frequencies).

fBm

Fractional Brownian motion (fBm) (II)

Additional properties

- A self-similar, stationary-increment process (H-SSSI).
- Its first order increments, $Y(n) = B(n+1) - B(n)$, are fractional Gaussian noise ▸ fGn, a stationary process with long-range dependence (LRD) for $\frac{1}{2} < H < 1$.
- Can be synthesized *efficiently* in 2D by introducing $\phi(\eta_1, \eta_2)$, autocorrelation of the increments ($O(N^2 \log N)$).

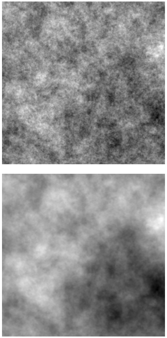

Figure: fBm for $H \in \{0.1, 0.6\}$

Is fBm sufficient as a prior?

Relevance as a model for NST

+ Gaussian.
+ Statistically self-similar.
- Behaviour determined by a single parameter, $H \in (0, 1)$.
- Isotropic in the statistical sense

$$R_B(M(x_1, y_2), M(x_1, y_2)) = R_B((x_1, y_2), (x_1, y_2))$$

for a rotation matrix M.
- Random phase – no edges in the usual sense.

$\Rightarrow$ May fit isotropic textures.

Isotropic texture

Anisotropic texture

▸ Statistics

Is fBm sufficient as a prior?

NSTs are of a broader class:

- Anisotropic.
- Phase and coherence properties.
- Containing both high-frequency details and long-range dependence (LRD).
- Possibly requiring more than one self-similarity parameter.

Isotropic texture

Anisotropic texture

Conclusion

A suitable model for NST should consist of a generalization of fBm to a more elaborate model.

Statistics

Example: Superresolution

NST super-resolution from a single image (I)

In a nutshell

- The problem:

$$\hat{X}(\eta_1, \eta_2) = \arg\min_{X} \left\| Y - \mathcal{D}(B * X) \right\|_2^2 + \lambda \phi(X)$$

- Our approach: Using *fBm* and *Phase*.

$$\begin{aligned} \hat{X} &= \alpha Y * H_{LP} + (1-\alpha) Z * H_{HP} && (11) \\ Z &\triangleq \mathcal{F}^{-1}\left\{ |\mathcal{F}\{W\}| \exp(j\angle\mathcal{F}\{Y\}) \right\} && (12) \\ \text{s.t.} \quad & \left\| Y - B\hat{X} \right\|_2 < \epsilon, \quad W \text{ is fBm} && (13) \end{aligned}$$

- Implementation via tensor diffusion yields the following scheme:

$$\begin{aligned} X_t = {} & 2(DB)^T(DBX - Y) - 2H(\hat{X}_{HP} - HX) + \\ & + \beta\nabla \cdot \left(\Psi'(|\nabla X + \alpha\nabla Y_\phi|^2)\nabla(X + \alpha Y_\phi)\right) \end{aligned}$$

The empirical image, $Y_\phi(\eta_1, \eta_2)$, has the following properties:

- A stochastic image, obtained from the empirical correlations of the degraded image, $Y(\eta_1, \eta_2)$.
- The correlations are suitable for the high-resolution image due to the self-similarity.

NST super-resolution from a single image (II)

LR image

Sparseness-based SR [Yang et al., 2008]

Proposed method

Ground truth

Outline

Long range dependence (LRD) in images

Determining LRD in random processes

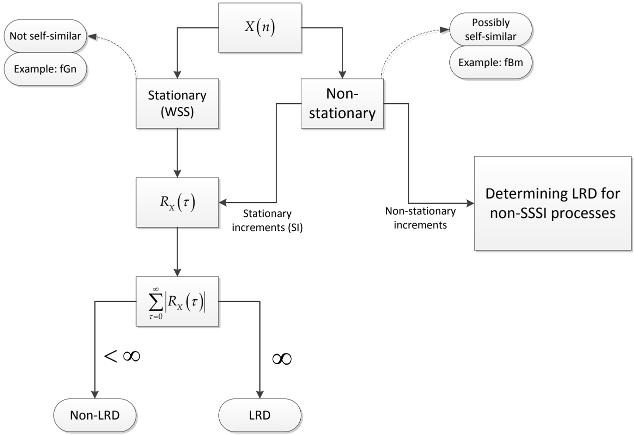

fGn

LRD in images

Determining LRD in random processes

Three types of interesting processes are considered:

1. Stationary with LRD (e.g., fGn).
   - Cannot be self-similar.
2. Self-similar with parameter H and stationary increments (H-SSSI).
   - $+$ Stationary increments $\Rightarrow$ Easy to analyze LRD and synthesize.
   - – Governed by a single parameter, H.
   - – LRD *only* on $H > 0.5$, where the process is smooth (persistent).
3. Self-similar *without* stationary increments.
   - $+$ More versatile; LRD is possible *with* non-smooth behaviour.
   - $+$ Governed by various self-similarity parameters, varying in space.
   - – More involved analysis and synthesis; how to determine LRD and H? How to synthesize efficiently? [Ayache et al., 2000, Pesquet-Popescu and Vehel, 2002]

$\star$ *Are NST H-SSSI?*

LRD in images

Determining LRD in random processes

⋆ Assuming images *are* H-SSSI (group 2).

Determining LRD of a signal $I(t)$ by:

$$W(t) \triangleq I(t) - I(t-1) \tag{14}$$

$$E[W(t)W(s)] = R_W(t,s) = R(\tau)|_{\tau=t-s}, \tau \in \mathbb{N} \tag{15}$$

$$L \triangleq \sum_{\tau=0}^{\infty} |R(\tau)| \tag{16}$$

L=∞ ⇒ LRD

In images, $I = I(x,y)$:

- Increments are calculated on both axes.
- The sum is evaluated on the 2D autocorrelation function.

LRD in images

Measuring LRD in images

- Autocorrelation shape: $R(r) = ar^{-b} + c$.
- Parameters $\{a, b, c\}$ found by curve fitting.

Results on Brodatz and McGill [Brodatz, 1966, A. Olmos and Kingdom, 2004]

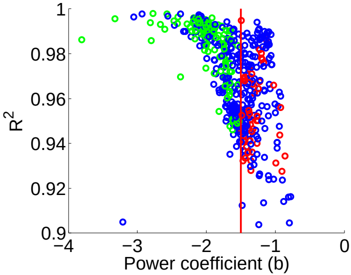

o Gaussian, non-LRD.

o Gaussian with LRD.

o Non Gaussian.

- Red line: fBm with $H = 0.5$.
- $a \approxeq 1$ and $c \approxeq 0$.
- Gaussianity is observed in 33% of the images.
- LRD+Gaussianity is observed in 10% of the images.

Expanding fBm

mBm - Multifractional Brownian motion

- Main concept: $H \rightarrow H(t)$ [Peltier and Levy-vehel, 1995].
- Covariance:

$$R_{W_H}(t,s) \propto |t|^{H(t)+H(s)} + |s|^{H(t)+H(s)} - |t-s|^{H(t)+H(s)} \tag{17}$$

Properties:

- Space-varying self-similarity.
- Long-range dependence for suitable functions $H(t)$, including high-frequency behaviour.
- Non-stationary increments (unlike fBm).
- Synthesis for $N \times N$ image:
  - Directly by covariance function, $O(N^6)$.
  - Approximately by N^2 fBm processes, $O(N^4 \log_2(N^2)^2)$.

  $\Rightarrow$ More complex than fBm.

$\star$ *Further analysis is required.*

Further properties

1. *Stochastic* properties: Discussed so far.
2. *Structured* properties: Phase.

The importance of the phase in images (I)

- ⋆ Phase is important for the visual appearance of images [Oppenheim and Lim, 1981].
- ⋆ Global v. Localized phase [Behar et al., 1992]

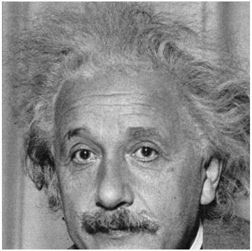

Einstein

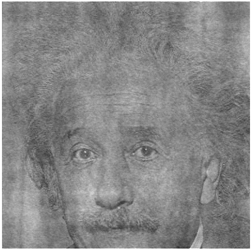

$\mathcal{F}^{-1}\{|Mandrill| \exp(j\angle Einstein)\}$

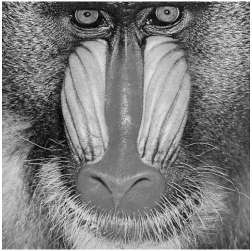

Mandrill

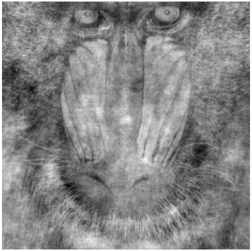

$\mathcal{F}^{-1}\{|Einstein| \exp(j\angle Mandrill)\}$

The importance of the phase in images (II)

$$Y = \mathcal{F}^{-1}\left\{|\mathcal{F}\{Y\}|e^{j\angle\mathcal{F}\{Y\}}\right\}$$

- Contour information is associated with spatial phase relationships ("in-phase"; "phase locked").
- Deviations in phase $\Rightarrow$ Distorted images.
- Phase quantization (reduction in number of bits) $\Rightarrow$ Compromise in image quality.
- In fBm, however, deviations in phase $\Rightarrow$ visually similar images.
- What is the role of phase in NST?
- A complete model should incorporate phase in the stochastic model.

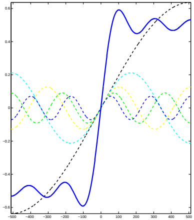

An edge and its decomposition

The importance of the phase in images (III)

Isotropic texture

Phase with $\sigma = 1$ normal distributed i.i.d noise (14.9dB PSNR)

- *Little* visual change in the case of isotropic textures.
- Isotropic textures - Random phase.
- Anisotropic textures - Phase info required.

The importance of the phase in images (III)

Anisotropic texture

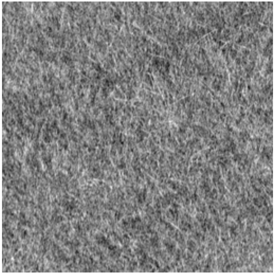

Phase with $\sigma = 1$ normal distributed i.i.d noise (18.1dB PSNR)

- ⋆ *Significant* contribution of phase info in the case of anisotropic textures.
- ⋆ Isotropic textures - Random phase.
- ⋆ Anisotropic textures - Phase info required.

Combining phase and random processes (I)

- Formulated as POCS

$$x_{k+1} = \mathcal{P}_{fBm}\left(\mathcal{P}_{phase}\left(x_k\right)\right) \tag{18}$$

- Is the projection functional convex?
- Can a process similar to reconstruction by phase and spatial constraints be developed?

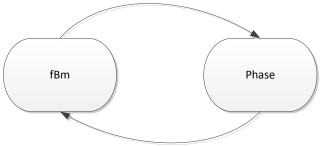

Combining phase and random processes (II)

Current study: A degradation model $Y = BX + N$, $\angle B = 0$ (zero phase)
Energy functional:

$$E(X) = \iint \left\| |\mathcal{F}\{X\}|^2 - |X_0|^2 \right\|_F^2 + \alpha \left\| \angle\mathcal{F}\{X\} - \angle Y \right\|_F^2 d\underline{x}, \qquad (19)$$

where X_0 has a Fourier magnitude similar to X. Using $\mathcal{F}\{X\} = A + jB$ we obtain:

$$E(A, B) = \iint \left\| A^2 + B^2 - |X_0|^2 \right\|_F^2 + \alpha \left\| \mathrm{atan2}(B, A) - \angle Y \right\|_F^2 d\underline{x}. \qquad (20)$$

E-L equations with gradient descend flow:

$$\partial_A L = 0, \partial_B L = 0 \qquad (21)$$

$$\Rightarrow \frac{d}{dt} A = \partial_A L, \frac{d}{dt} B = \partial_B L \qquad (22)$$

- Covnergence guarantees?
- Optimizing for a desired magnitude or phase.
- Variational approach: Regularization and fidelity terms are easy to incorporate.

Example

Towards a universal stochastic texture model

The model should include:

- Stochastic characteristics (fBm, mBm): Self similarity ($\{\boldsymbol{H}_i\}$), LRD, specific rate of decay of the covariance of various subclasses of stocastic textures.
- Phase dependency:
  - Local phase.
  - Orientation – θ
  - Coherence – μ

Representation via a manifold:

$$(\eta_1, \eta_2) \rightarrow (\eta_1, \eta_2, \boldsymbol{H}_i, \theta, \mu, \cdots). \tag{23}$$

Textures as a manifold, embedded in a suitable space [Kimmel et al., 2000].
Advantages:

- Natural representation for various features, including color.
- A measure of similarity between two textures via the intrinsic metric.

Further research: Summary

Main objective: A complete model for NST

1. Obtaining a fractal, stochastic model with LRD and high-frequency behaviour.
2. Obtaining a suitable model for the phase of NST.
3. Combining the two models to a unified NST model.

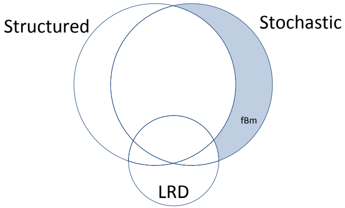

Further expansions and applications

Segmentation

- Classifying textured and non-textured areas in an image.
- Classifying textures according to covariance properties.

Multiband decomposition

- Images containing a “layer” of NST over a cartoon or different texture type image.
- Using known methods for decompositions [Starck et al., Gilboa]. Enhancing the NST while the rest is done by known models for cartoon images.

Applications

- Relevance for medical images exhibiting fractal properties.

Outline

Statistics and abundance of NST [Zachevsky and Zeevi, 2014]

1. Are NST indeed Gaussian and self-similar?
2. Are NST abundant in natural images?

Test method:

- Test set: VisTex [Pickard et al., 1995].
- Number of images: **1914** 256×256 images of textures; cartoon, structured and NST taken arbitrarily from the database.
- Distribution: Generalized Gaussian

$$f(x) = \frac{1}{C(\alpha, \beta)} e^{-(|x-\mu|/\alpha)^{\beta}} \tag{24}$$

  - Normal distribution for $\beta = 2$.
  - Leptokurtic for $0 < \beta < 2$.
  - Shown to model leptokurtic behaviour of natural images for $\beta \in [0.5, 1]$ [Srivastava et al., 2003, Simoncelli and Adelson, 1996].

Gaussianity

Gaussianity evaluated in two methods:

1. Estimating $\hat{\alpha}_{ML}$ and $\hat{\beta}_{ML}$ for the generalized Gaussian and using KL divergence for the former and normal distributions against the empirical distribution.
2. Estimating $\hat{\beta}_{ML}$ (controlling kurtosis) and comparing result with known values of β for natural images.

$$K = \frac{\Gamma(5/\beta)\Gamma(1/\beta)}{\Gamma(3/\beta)^2} - 3. \tag{25}$$

Results:

1. **620**/**1914** images (**32**%) with lower KL divergence for normal distribution.
2. **19**% of the images with kurtosis values more suitable to Gaussian.

Self-similarity

Evaluating self-similarity in Gaussian processes:

1. Assume $B(t)$ is Gaussian and self-similar.
2. Then, $B(t)$ is fBm with a parameter H and its increments variance is known.

Let $W_{H,\tau}(t) = B_H(t+\tau) - B_H(t)$ be the increments of the fBm $B_H(t)$. Then,

$$\operatorname{var}(W_{H,\tau}(t)) = \sigma_B^2 \cdot \tau^{2H}. \tag{26}$$

Performing log-regression on the increments:

$$y_H(\tau) = 2Hx(\tau) + b_H. \tag{27}$$

Result: Median R^2 value of 0.96 - indicating self-similarity.

Conclusion

Judging by the test set, many images have Gaussian and self-similar statistics, rather than non-Gaussian.

⋆ Performed on entire images without segmentation for different textures.

Outline

Introduction

Super-resolution (SR) problem formulation:

$$Y(\eta_1, \eta_2) = \mathcal{D}\left((B * X)(\eta_1, \eta_2)\right)$$

Degradation caused by decimation and blur

- Decimation, $\mathcal{D}$, causes aliasing in finitely supported (typically small) PSFs.
- Blur kernel, $B(\eta_1, \eta_2)$: Gaussian, averaging, ...


Original image


Blurred image


BM3D Reconstructed


Blurred+subsampled


BM3D Reconstructed

BM3D is a sparsity-based deblurring algorithm [Danielyan et al., 2012].

Introduction

Super-resolution (SR) problem formulation:

$$Y(\eta_1, \eta_2) = \mathcal{D}\left((B * X)(\eta_1, \eta_2)\right)$$

Degradation caused by decimation and blur

- Decimation, $\mathcal{D}$, causes aliasing in finitely supported (typically small) PSFs.
- Blur kernel, $B(\eta_1, \eta_2)$: Gaussian, averaging, ...

Original image

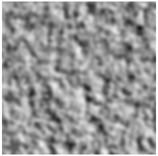

Blurred image

BM3D Reconstructed

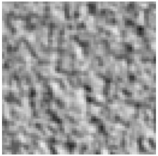

Blurred+subsampled

BM3D Reconstructed

BM3D is a sparsity-based deblurring algorithm [Danielyan et al., 2012].

Super-resolution

The super-resolution problem

- Multi-frame super-resolution: Given $\{Y_i(\eta_1, \eta_2)\}_{i=1}^{N}$ [Irani and Peleg, 1990, Elad and Feuer, 1997, Yang and Huang, 2010], ...
- Single-frame super-resolution (upscaling): Given a single measurement, $N = 1$ [Freeman et al., 2002, Glasner et al., 2009, Gilboa et al., 2002, Zeyde et al., 2011]
  - *The goal: Restore a high-resolution image from a single blurred and subsampled observation.*

Texture enhancement

Super-resolution as a specific problem in image enhancement

- Cartoon v. textures – non bounded-variation (BV) space [Gousseau and Morel, 2001]

Methods for texture enhancement

- Differential equations, $I_t = \nabla \cdot (g(|\nabla I|)\nabla I)$ [Gilboa et al., 2002]
  - TeD [Ratner and Zeevi, 2011]
  - Complex diffusion with potential [Honigman and Zeevi, 2006]
- Sparseness-based, $X = D\alpha + V$ [Yang et al., 2010]
- Example (learning)-based superresolution [Freeman et al., 2002]
  - Single-image example-based [Glasner et al., 2009]
- Texture synthesis [Efros and Leung, 1999]
- Manifold-geometry based [Kimmel et al., 2000]

Relevance and contribution

Further research is called for in analysis and enhancement of textured images

Theoretical model

- Analysis of natural images as realizations of random processes
- Interest in the underlying model

Better models $\Rightarrow$ better enhancement algorithms

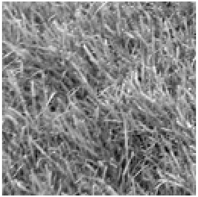

Original image

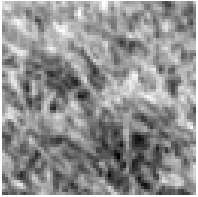

Degraded image

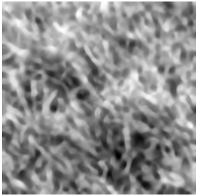

SR [Freeman et al., 2002]

Regularization

Required for solving SR as an ill-posed problems

$$\hat{X}(\eta_1, \eta_2) = \arg\min_X \left\| Y - \mathcal{D}(B * X) \right\|_2^2 + \lambda \phi(X)$$

Common regularization functions:

- L_2-based: high gradients are not common, $\phi(x) = \left\| \nabla X \right\|_2^2$
- TV-based: promotes piecewise-smooth segments $\phi(x) = \left\| \nabla X \right\|_1$
- L_p norms, for $p \in (1, 2)$
- L_0 pseudo-norm, promotes sparsity: $\phi(\alpha) = \|\alpha\|_0$, $X = D\alpha + V$
- Reflect an image model (BV space).

Issues:

- Restoration results in cartoon images
- Textured details are lost

Stochastic texture model

Exploiting the self-similarity

NSTs are statistically self-similar and the distributions are scale invariant.

1. The degraded image, $Y(\eta_1, \eta_2) = DBX(\eta_1, \eta_2)$, has similar distribution as $X(\eta_1, \eta_2)$.
2. 1D and 2D increments' statistics contain valuable information.
3. Generalizing the fBm model to nonstationary fields with stationary increments
4. Build an *empirical image* from $Y(\eta_1, \eta_2)$ using a structure function.

Exploiting the fBm model

Possible options - noiseless case:

- MMSE estimation: $\hat{X} = E[X|Y] = E[X|Y = \mathcal{D}(B * X)]$
  - Not suitable for noiseless, ill-posed problems.
  - L_2 based optimization.
- MAP estimation: $\hat{X} = \arg\max P(X|Y)$

$$\hat{X} = ((DB)^T(DB))^{-1}(DB)^T y \quad (28)$$

- Another approach: Using *Phase*.

$$\hat{X} = \alpha Y * H_{LP} + (1-\alpha) Z * H_{HP} \quad (29)$$

$$Z \triangleq \mathcal{F}^{-1}\{|\mathcal{F}\{W\}| \exp(j\angle\mathcal{F}\{Y\})\} \quad (30)$$

$$\text{s.t.} \quad \left\| Y - B\hat{X} \right\|_2 < \epsilon, \quad W \text{ is fBm} \quad (31)$$

Phase of a frequency response

$$Y = \mathcal{F}^{-1}\left\{|\mathcal{F}\{Y\}|e^{j\angle\mathcal{F}\{Y\}}\right\}$$

- Specific image information is contained in the phase.
- Magnitudes contain common information, characteristic of a general class of images.
- The phase is not affected by blurring.

Proposal

Use the phase from the degraded image and the magnitude from the fBm generalized spectrum.

- Better in terms of visual assessment.
- Phase matching and optimization.

Visual example

$$X = \underbrace{X_{LP} + \hat{X}_{HP}}_{\hat{X}} + V,$$

where

$$\hat{X}_{HP}(\eta_1, \eta_2) = f(\omega, X_{LP})$$

- $X_{LP}(\eta_1, \eta_2)$ is a low-frequency, degraded, image
- $X_{HP}(\eta_1, \eta_2)$ is composed from $\angle X_{LP}$ and an fBm image, $B_H(\eta_1, \eta_2)$
- The high frequencies are obtained from fBm representation of the degraded image

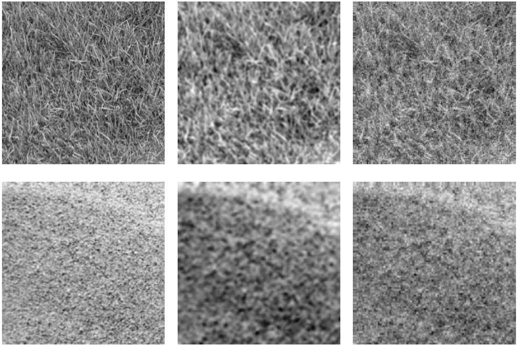

Original image | $X_{LP}(\eta_1, \eta_2)$ | $\hat{X}(\eta_1, \eta_2)$

Implementation: Tensor diffusion

Basic reaction-diffusion equation for deblurring [Welk et al., 2005]:

$$\begin{aligned}
\mathcal{L}(X) &= \left\| Y - DBX \right\|^2 + \underbrace{\lambda\Psi(\nabla X)}_{\text{Regularization}} \\
\hat{X} &= \arg\min_X \left\| Y - DBX \right\|^2 + \lambda\Psi(\nabla X) \\
X_t &= \underbrace{-(DB)^T(DBX - Y)}_{\text{Reaction}} + \underbrace{\lambda\nabla \cdot (T(\nabla X)\nabla X)}_{\text{Diffusion}} \\
T &= (\omega_1, \omega_2) \begin{pmatrix} \lambda_1 & 0 \\ 0 & \lambda_2 \end{pmatrix} \begin{pmatrix} \omega_1 \\ \omega_2 \end{pmatrix}
\end{aligned}$$

where

$$\omega_1 || \nabla X, \quad \omega_2 \perp \nabla X$$

- Performs *anisotropic* diffusion, used in various image enhancements tasks.
- Applies different diffusion coefficients, according to orientation.

Modified tensor diffusion for texture enhancement

Incorporation of the model into the PDE

- Modified reaction term: $\left(X_{HP} - \hat{X}_{HP}\right)^2$, recovers degraded high frequencies
- Diffusion tensor *modified*: $T\left(\nabla\left(X + \alpha Y_\phi\right)\right)$, preserves texture orientation

New scheme:

$$
\begin{aligned}
X_t &= 2(DB)^T(DBX - Y) - 2H(\hat{X}_{HP} - HX) + \\
&\quad + \beta\nabla\cdot(\Psi'(|\nabla X + \alpha\nabla Y_\phi|^2)\nabla(X + \alpha Y_\phi))
\end{aligned}
$$

The empirical image, $Y_\phi(\eta_1, \eta_2)$, has the following properties:

- A stochastic image, obtained from the empirical correlations of the degraded image, $Y(\eta_1, \eta_2)$.
- The correlations are suitable for the high-resolution image due to the self-similarity.

Modified tensor diffusion for texture enhancement

Stopping condition

- How to set a stopping condition?
- Chosen criteria: Hurst parameter.
- For a 2D-fBm, The original (high-resolution) Hurst parameter can be estimated via the degraded image. [Zachevsky and Zeevi, 2013b]

Results

- Performs well on isotropic stochastic textures.
- Recovers missing details according to the model.
- PSNR or MSE-based comparison methods not applicable ($PSNR < 20[dB]$)

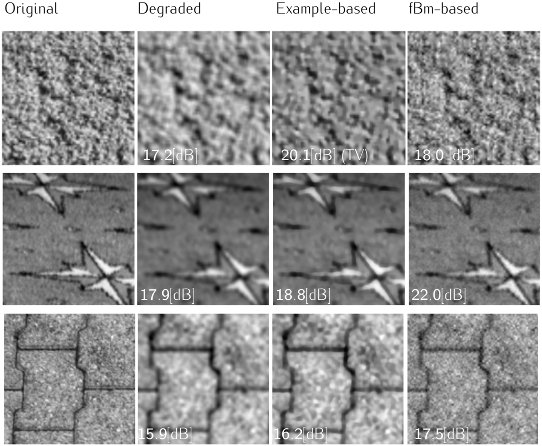

[Zachevsky and Zeevi, 2013a]

Results

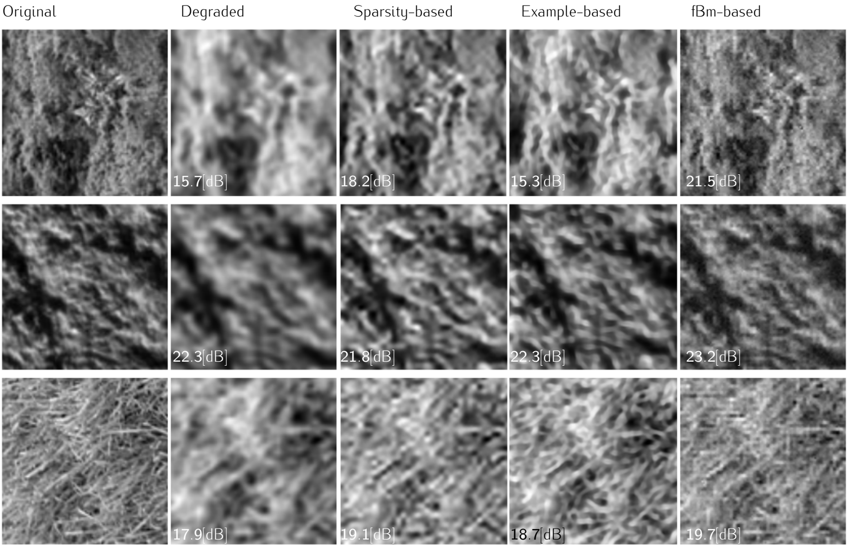

[Zeyde et al., 2011]

Bibliography I

Javier Portilla, Vasily Strela, Martin J Wainwright, and Eero P Simoncelli. Image denoising using scale mixtures of Gaussians in the wavelet domain. *Image Process. IEEE Trans.*, 12(11):1338–1351, January 2003. ISSN 1057-7149. doi: 10.1109/TIP.2003.818640. URL **http://www.ncbi.nlm.nih.gov/pubmed/18244692**.

A Srivastava, A B Lee, and E P Simoncelli. On Advances in Statistical Modeling of Natural Images. *J. Math. Imaging Vis.*, 18:17–33, 2003.

Patrick Perez. Markov Random Fields and Images. 11(4):413–437, 1998.

Stan Z Li. *Markov random field modeling in image analysis*. Springer, 2009.

Daniel Zoran. Natural Images , Gaussian Mixtures and Dead Leaves. pages 1–9, 2012.

Stefan Roth and Michael J. Black. Fields of Experts. *Int. J. Comput. Vis.*, 82(2):205–229, January 2009. ISSN 0920-5691. doi: 10.1007/s11263-008-0197-6. URL **http://link.springer.com/10.1007/s11263-008-0197-6**.

Michael Elad and Mario A T Figueiredo. On the Role of Sparse and Redundant Representations in Image Processing. *Proc. IEEE*, 98(6):972–982, June 2010. ISSN 0018-9219. doi: 10.1109/JPROC.2009.2037655. URL **http://ieeexplore.ieee.org/lpdocs/epic03/wrapper.htm?arnumber=5420029**.

Ido Zachevsky and Yehoshua Y Zeevi. On the statistics of natural stochastic textures and their application in image processing. In *ICASSP2014 (Submitted)*, Florence, Italy, 2014.

Carlos M. Jarque and Anil K. Bera. Efficient tests for normality, homoscedasticity and serial independence of regression residuals. *Econ. Lett.*, 6(3):255–259, January 1980. ISSN 01651765. doi: 10.1016/0165-1765(80)90024-5. URL **http://linkinghub.elsevier.com/retrieve/pii/0165176580900245**.

Yulia R. Gel and Joseph L. Gastwirth. A robust modification of the JarqueâĂŞBera test of normality. *Econ. Lett.*, 99(1): 30–32, April 2008. ISSN 01651765. doi: 10.1016/j.econlet.2007.05.022. URL **http://linkinghub.elsevier.com/retrieve/pii/S0165176507001838**.

Ido Zachevsky and Yehoshua Y Zeevi. Single-image superresolution of self-similar textures. In *IEEE Int. Conf. Image Process.*, pages 952–956, September 2013a.

Gennady Samorodnitsky. Long memory and self-similar processes. pages 1–12, 2005.

Bibliography II

K B Eom. Long-correlation image models for textures with circular and elliptical correlation structures. *IEEE Trans. Image Process.*, 10(7):1047–55, January 2001. ISSN 1057-7149. doi: 10.1109/83.931099. URL **http://www.ncbi.nlm.nih.gov/pubmed/18249678**.

B. Pesquet-Popescu and J. L Vehel. Stochastic fractal models for image processing. *IEEE Signal Process. Mag.*, 19(5): 48– 62, September 2002. ISSN 1053-5888. doi: 10.1109/MSP.2002.1028352. URL **http://ieeexplore.ieee.org/ielx5/79/22084/01028352.pdf?tp=&arnumber=1028352&isnumber=22084**.

R.L. Kashyap and P.M. Lapsa. Synthesis and Estimation of Random Fields Using Long-Correlation. (6):800–809, 1984.

Guy Gilboa and Stanley Osher. Nonlocal operators with applications to image processing. *Multiscale Model. Simul.*, 7(3):1005–1028, 2008.

Benoit B Mandelbrot and John W Van Ness. Fractional Brownian motions, fractional noises and applications. *SIAM Rev.*, 10(4):422–437, 1968.

Andrei N Kolmogorov. Wienersche Spiralen und einige andere interessante Kurven im Hilbertschen Raum. In *CR Acad. Sci. URSS*, volume 26, pages 115–118, 1940.

Jianchao Yang, John Wright, Yi Ma, and Thomas Huang. Image super-resolution as sparse representation of raw image patches. In *IEEE Conf. Comput. Vis. Pattern Recognit.*, pages 1–8, June 2008. ISBN 978-1-4244-2242-5. doi: 10.1109/CVPR.2008.4587647. URL **http://ieeexplore.ieee.org/lpdocs/epic03/wrapper.htm?arnumber=4587647**.

A. Ayache, S. Cohen, and J.L. Vehel. The covariance structure of multifractional Brownian motion, with application to long range dependence. *2000 IEEE Int. Conf. Acoust. Speech, Signal Process. Proc.*, 6:3810–3813, 2000. doi: 10.1109/ICASSP.2000.860233. URL **http://ieeexplore.ieee.org/lpdocs/epic03/wrapper.htm?arnumber=860233**.

Phil Brodatz. *Textures: a photographic album for artists and designers*, volume 66. Dover New York, 1966.

A. Olmos and F. A. A. Kingdom. A biologically inspired algorithm for the recovery of shading and reflectance images. *Perception*, 33:1463—-1473, 2004.

Romain Francois Peltier and Jacques Levy-vehel. Multifractional Brownian motion: definition and preliminary results. Technical report, 1995.

Alan v. Oppenheim and Jae S. Lim. Importance of Phase in Signals. *Proc. IEEE*, 69(5):529–541, 1981.

Bibliography III

Jacques Behar, Moshe Porat, and Yehoshua Y Zeevi. Image Reconstruction from Localized Phase. *IEEE Trans. Signal Process.*, 40(4):736–743, 1992.

Ron Kimmel, Nir A Sochen, and Ravi Malladi. On the Geometry of Texture. Technical report, 2000.

J Starck, Dapnia Sedi-sap, Service Astrophysique, C E A Saclay, and Gif Yvette. Morphological Component Analysis.

Guy Gilboa. A Spectral Approach to Total Variation.

R Pickard, C Graszyk, S Mann, J Wachman, L Pickard, and L Campbell. Vistex database. *Media Lab., MIT, Cambridge, Massachusetts*, 1995.

Eero P Simoncelli and Edward H Adelson. Noise removal via Bayesian wavelet coring. In *Image Process. Int. Conf.*, pages 379–382, 1996. ISBN 078033258X.

Aram Danielyan, Vladimir Katkovnik, and Karen Egiazarian. BM3D frames and variational image deblurring. *IEEE Trans. Image Process.*, 21(4):1715–1728, April 2012. ISSN 1941-0042. doi: 10.1109/TIP.2011.2176954. URL `http://www.ncbi.nlm.nih.gov/pubmed/22128008`.

Michal Irani and Shmuel Peleg. Super resolution from image sequences. In *Pattern Recognition, 1990. Proceedings., 10th Int. Conf.*, volume 2, pages 115–120. IEEE Comput. Soc. Press, June 1990. ISBN 0-8186-2062-5. doi: 10.1109/ICPR.1990.119340. URL `http://ieeexplore.ieee.org/lpdocs/epic03/wrapper.htm?arnumber=119340`.

Michael Elad and Arie Feuer. Restoration of a single superresolution image from several blurred, noisy, and undersampled measured images. *IEEE Trans. Image Process.*, 6(12):1646–1658, January 1997. ISSN 1057-7149. doi: 10.1109/83.650118. URL `http://www.ncbi.nlm.nih.gov/pubmed/18285235`.

Jianchao Yang and Thomas Huang. Image super-resolution: Historical overview and future challenges. In *Super-resolution imaging*. Boca Raton, FL: CRC Press, 2010.

William T Freeman, Thouis R Jones, and Egon C Pasztor. Example-Based Super-Resolution. *Comput. Graph. Appl. IEEE*, 22(2):56–65, 2002.

Daniel Glasner, Shai Bagon, and Michal Irani. Super-resolution from a single image. In *2009 IEEE 12th Int. Conf. Comput. Vis.*, pages 349–356, September 2009. ISBN 978-1-4244-4420-5. doi: 10.1109/ICCV.2009.5459271. URL `http://ieeexplore.ieee.org/lpdocs/epic03/wrapper.htm?arnumber=5459271`.

Bibliography IV

Guy Gilboa, Nir Sochen, and Yehoshua Y Zeevi. Forward-and-backward diffusion processes for adaptive image enhancement and denoising. *IEEE Trans. Image Process.*, 11(7):689–703, January 2002. ISSN 1057-7149. doi: 10.1109/TIP.2002.800883. URL **http://www.ncbi.nlm.nih.gov/pubmed/18244666**.

Roman Zeyde, Michael Elad, and Matan Protter. On Single Image Scale-Up Using Sparse-Representations. In *Curves and Surfaces*, number 1, pages 711–730. 2011.

Yann Gousseau and Jean-Michel Morel. Are Natural Images of Bounded Variation? *SIAM J. Math. Anal.*, 33(3): 634–648, January 2001. ISSN 0036-1410. doi: 10.1137/S0036141000371150. URL **http://epubs.siam.org/doi/abs/10.1137/S0036141000371150**.

Vadim Ratner and Yehoshua Y Zeevi. Denoising-enhancing images on elastic manifolds. *IEEE Trans. Image Process.*, 20(8):2099–109, August 2011. ISSN 1941-0042. doi: 10.1109/TIP.2011.2118221. URL **http://www.ncbi.nlm.nih.gov/pubmed/21342847**.

Ori Honigman and Yehoshua Y. Zeevi. Enhancement of Textured Images Using Complex Diffusion Incorporating Schrodinger's Potential. In *IEEE Int. Conf. Acoust. Speech Signal Process.*, pages 633–636, May 2006.

Jianchao Yang, John Wright, Thomas Huang, and Yi Ma. Image Super-Resolution via Sparse Representation. *Image Process. IEEE Trans.*, 19(11):2861–2873, May 2010. ISSN 1941-0042. doi: 10.1109/TIP.2010.2050625. URL **http://www.ncbi.nlm.nih.gov/pubmed/20483687**.

Alexei A Efros and Thomas K Leung. Texture synthesis by non-parametric sampling. In *Proc. 7th IEEE Int. Conf. Comput. Vis.*, volume 2, pages 1033–1038. Ieee, 1999. ISBN 0-7695-0164-8. doi: 10.1109/ICCV.1999.790383. URL **http://ieeexplore.ieee.org/lpdocs/epic03/wrapper.htm?arnumber=790383**.

Martin Welk, David Theis, Thomas Brox, and Joachim Weickert. PDE-based deconvolution with forward-backward diffusivities and diffusion tensors. *Scale Sp. PDE Methods Comput. Vis.*, pages 585–597, 2005. URL **http://link.springer.com/chapter/10.1007/11408031_50**.

Ido Zachevsky and Yehoshua Y. Zeevi. Superresolution of self-similar textures. *CCIT Rep. #838. EE Pub, Tech. Isr. Inst. Technol.*, 1795, 2013b.

Stephan Hoefer, H Hannachi, Madhukar Pandit, and Ramdas Kumaresan. Isotropic Two-Dimensional Fractional Brownian Motion and its Application in Ultrasonic Analysis. In *Eng. Med. Biol. Soc. 1992 14th Annu. Int. Conf. IEEE*, pages 1267–1269, November 1992. ISBN 0780307852.

Bibliography V

Lance M Kaplan and C-CJ Kuo. An improved method for 2-D self-similar image synthesis. *IEEE Trans. Image Process.*, 5(5):754–761, January 1996. ISSN 1057-7149. doi: 10.1109/83.495958. URL `http://www.ncbi.nlm.nih.gov/pubmed/18285164`.

Pietro Perona and Jitendra Malik. Scale-space and edge detection using anisotropic diffusion. *IEEE Trans. Pattern Anal. Mach. Intell.*, 12(7):629–639, July 1990. ISSN 01628828. doi: 10.1109/34.56205. URL `http://ieeexplore.ieee.org/lpdocs/epic03/wrapper.htm?arnumber=56205`.

Joachim Weickert. *Anisotropic Diffusion in Image Processing*. Teubner Stuttgart, 1998.

Béatrice Pesquet-Popescu and Pascal Larzabal. Synthesis of nonstationary fields with stationary increments. In *Image Process. Its Appl. Sixth Int. Conf.*, volume 1, pages 303–307, July 1997.

Wen-Chieh Lin, James Hays, Chenyu Wu, Vivek Kwatra, and Yanxi Liu. A comparison study of four texture synthesis algorithms on regular and near-regular textures. Technical report, Carnegie Mellon University, 2004.

Michael F Barnsley. *Fractals everywhere*, volume 19. Academic Press Professional, Inc., 1988.

Thank you

Backup

Outline

Nomenclature

NST	Natural stochastic textures.
H	Hurst parameter.
SS	Self-similar.
WSS	Wide-sense (weak) stationarity.
H-SSSI	Self-similar with a parameter H and stationary increments.
LRD	Long-range dependence.
fBm	Fractional Brownian motion.
fGn	Fractional Gaussian noise.
mBm	Multifractional Brownian motion.
GMM	Gaussian mixture models.
MRF	Markov random fields.
FoE	Field of Experts.

Fractional Brownian motion synthesis

1. Naive [Hoefer et al., 1992]: Construct $R_B(t,s)$, the autocorrelation function of the fBm:

$$\begin{aligned} E\left[B_H(t)B_H(s)\right] &= \frac{\sigma^2}{2}\left(|t|^{2H}+|s|^{2H}-|t-s|^{2H}\right) \\ \sigma^2 &= \frac{\sigma_B^2}{2}\frac{\cos(\pi H)}{\pi H}\Gamma(1-2H) \end{aligned}$$

   Inefficient due to use of Cholesky decomposition.

2. Via the Fourier domain [Kaplan and Kuo, 1996]:
   - First- and second-order increments are stationary.
   - Their autocorrelations are expressed via a structure function, $\phi(\eta_1, \eta_2)$.
   - Fields with these autocorrelation functions can be efficiently synthesized via the Fourier domain.
   - 2D fBm is obtained by summation of the increments.

Back

Anisotropic diffusion

Non-linear *isotropic* diffusion [Perona and Malik, 1990]

$$X_t = \nabla \cdot (g(|\nabla X_\sigma|)\nabla X)$$
$$g(s^2) = \frac{1}{1+\left(\frac{s^2}{K^2}\right)}$$

- Adaptive: diffusion coefficient inversely proportional to norm of gradient
- Done isotropically, regardless of orientation

Weickert anisotropic diffusion [Weickert, 1998]:

$$X_t = \nabla \cdot (D(\nabla X)\nabla X)$$
$$D = (\omega_1, \omega_2)\begin{pmatrix}\lambda_1 & 0\\ 0 & \lambda_2\end{pmatrix}\begin{pmatrix}\omega_1\\ \omega_2\end{pmatrix}$$

- For edge preserving denoising: λ_1 similar to Perona and Malik, and λ_2=0.1. Enhances edges according to orientation.

Back

Modified diffusion equation

- A nonstationary field with stationary increments can be synthesized using a generating (structure) function, $\phi(\eta_1, \eta_2)$ [Pesquet-Popescu and Larzabal, 1997]:

$$\begin{aligned} \phi(\Delta_1, \Delta_2) &= var\left(F(\eta_1, \eta_2) - F(\eta_1 - \Delta_1, \eta_2 - \Delta_2)\right) \\ \phi_{fBm}(\Delta_1, \Delta_2) &= (\Delta_1^2 + \Delta_2^2)^H \triangleq r^{2H} \end{aligned}$$

- The empirical image, $Y_\phi(\eta_1, \eta_2)$, is obtained by an inverse process using an empirical structure function.

$$\hat{\phi}(\eta_1, \eta_2) = f_1(Y(\eta_1, \eta_2)) \quad \Rightarrow \quad \hat{B}_{\hat{\phi}}(\eta_1, \eta_2) = f_2(\hat{\phi}, \omega)$$

- Due to the self similarity, the correlations are suitable for the superresolution image.

Modified diffusion equation

- The inverse process is performed via solving an ill-posed least squares problem:

$$\underline{\phi} = \arg\min_{\underline{x}} \left\| D\underline{x} - \underline{r} \right\|_2$$

- Further methods can be explored to find more suitable empirical structure functions.

Example:

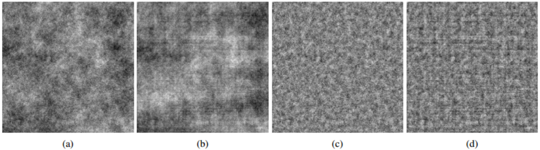

Figure: Original fBm, fBm from $\phi(\eta_1, \eta_2)$ and high-pass versions

Back

Empirical function in algorithm progress

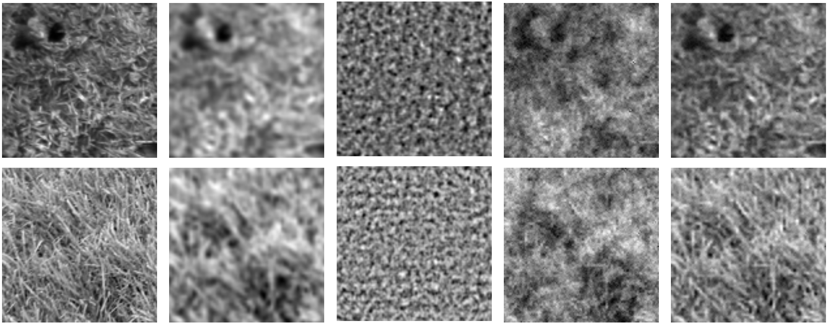

Original image | Degraded image | $Y_\phi(\eta_1, \eta_2)$ | $\hat{X}(\eta_1, \eta_2)$ | Enhanced image

- Further study necessary for empirical image. Back

Can fBm be learned?

- If an image is Gaussian and SSSI, fBm fits.
- Gaussian statistics $\Rightarrow$ fits for GMM. Or does it?
- Can it be learned from samples? WLLN $\Rightarrow$ Yes. But:
  - Expectation-Maximization used for GMM.
  - EM "learns" stationary (Toeplitz) covariance matrices.
  - Nonstationary.

$$\Lambda^* = \sum_{i=1}^{N} xx^T \tag{32}$$

About Gaussianity (I)

A possible estimator: MAP
For example, $y = Wx + n$, where $n \sim \mathcal{N}(0, \sigma_N^2 I), x \sim \mathcal{N}(0, \Sigma)$.

$$\begin{aligned} \hat{x} &= \arg\max_x P(x|y) && (33) \\ &= \arg\min_x \left\|y - Wx\right\|_2^2 + \sigma_N^2 x^T \Lambda^{-1} x && (34) \\ &= \arg\min_x \left(-W^T y\right)^T x + \frac{1}{2} x^T \left(W^T W + \sigma_N^2 \Sigma^{-1}\right) x && (35) \end{aligned}$$

$\Rightarrow$ A quadratic programming problem.

However, in the case of $\sigma_N^2 \approxeq 0$, we obtain:

$$\begin{aligned} 0 &= W^T (W\hat{x} - y) && (36) \\ \hat{x} &= (W^T W)^{-1} W^T y && (37) \end{aligned}$$

About Gaussianity (II)

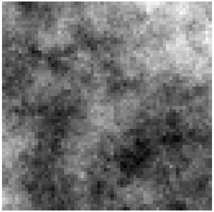

Original image

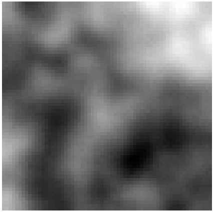

Blurred with $\sigma_B = 4$, 1% noise.

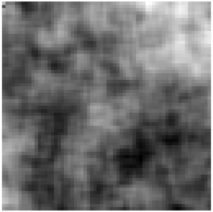

Result

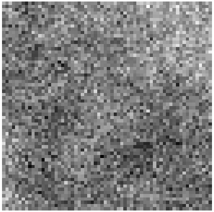

Noisy with 50% noise, $\sigma_B = 0.5$.

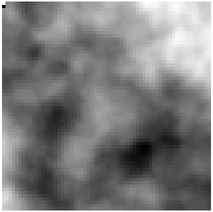

Result

LRD example: fractional Gaussian noise (fGn)

This is a *stationary* process that exhibits long-range dependencies

Let $W_H(n)$ be fGn. Then:

- Autocorrelation:
  $E[W_H(t)W_H(s)] = r(t-s) \triangleq r(k) \propto (k+1)^{2H} + |k-1|^{2H} - 2k^{2H}$.
- In the limit of $k \to \infty$, $r(k) \propto k^{-2(1-H)}$.
- LRD for $\frac{1}{2} < H < 1$.
- Obtained as the increments of an fBm: $W_H(n) = B_H(n+1) - B_H(n)$, $B_H(n)$ is fBm.

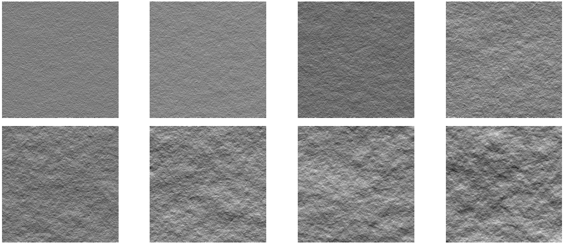

Stationary for any $H \in (0,1)$.

Texture properties

Types of textures [Lin et al., 2004]

- Regular (structured): pattern-based
- Stochastic: based on random processes, $X(\eta_1, \eta_2) = X(\eta_1, \eta_2, \omega)$

- Realizations of a random process
- Self-similar, $X_c(at) \overset{d}{=} |a|^c X_c(t)$ (Fractal properties [Barnsley, 1988])
- Long-range dependences [Gilboa and Osher, 2008, Eom, 2001, Pesquet-Popescu and Vehel, 2002, Kashyap and Lapsa, 1984]

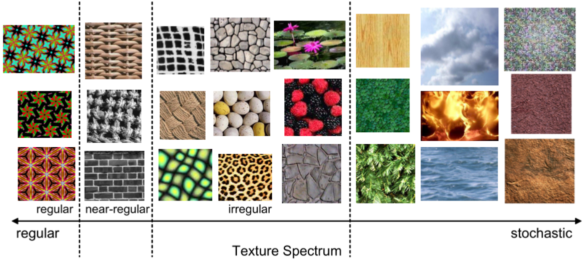

Figure: Textures spectrum [Lin et al., 2004]

FBm intuitive explanation in 1D

- Brownian motion is the the scaling limit of random walk:

$$X_{n+1} = X_n + W_n, \tag{38}$$

where W_n is i.i.d.

  - ⋆ Each step is independent of the previous one.

- In Fractional Brownian motion, W_n is stationary but *not* independent.
  - ⋆ For $H > 0.5$ the increments are *positively correlated*, and adjacent steps will tend to be in the *same direction*.
  - ⋆ For $H < 0.5$ the increments are *negatively correlated*, and adjacent steps will tend to be in *opposite directions*.

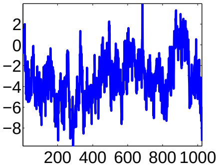

$H = 0.2$

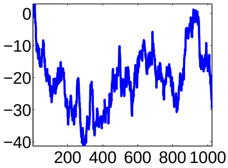

$H = 0.5$

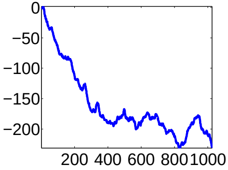

$H = 0.8$

Brodatz and McGill image banks

Randomly chosen examples [Brodatz, 1966, A. Olmos and Kingdom, 2004]

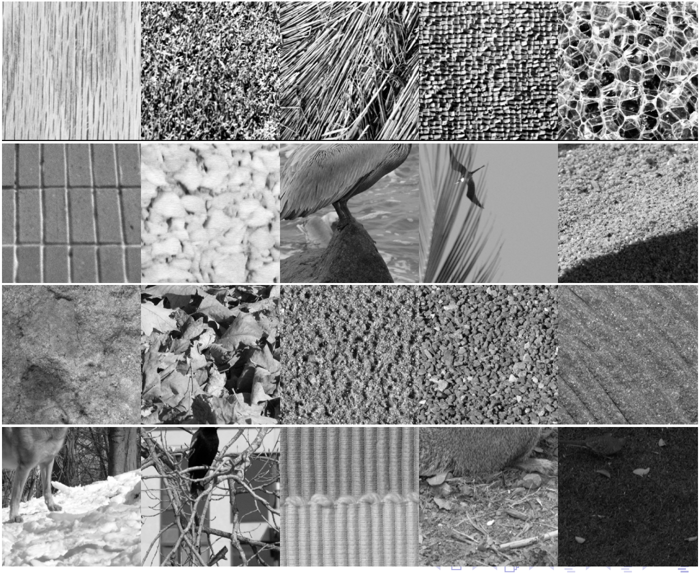

2D image histogram

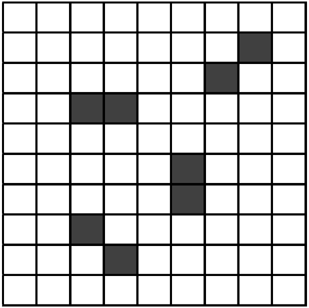

⋆ The histogram is evaluated on pairs of adjacent pixels.

Phase and random processes: Preliminary results

- Using the proposed scheme with the oracle autocorrelation.

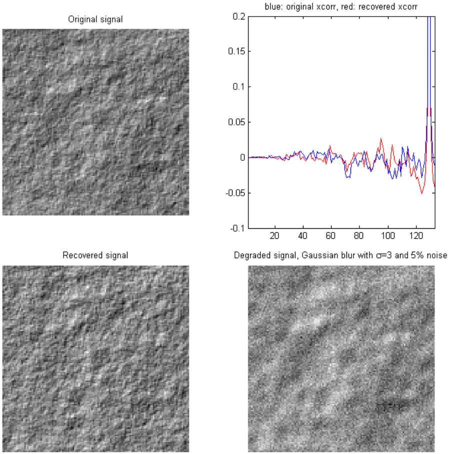

Is fBm sufficient as a prior?

Empirical distributions:

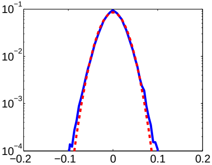

Marginal

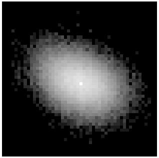

Joint

Isotropic texture

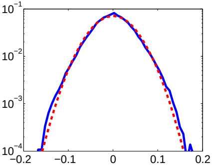

Marginal

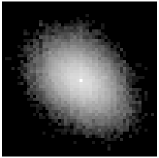

Joint

Anisotropic texture

Modified diffusion equation

Visualizing the two additions (zoomed-in images)

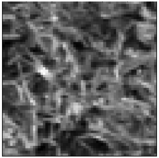

Original image

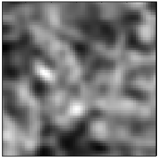

Degraded image

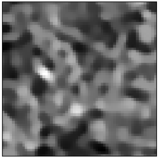

Original PDE

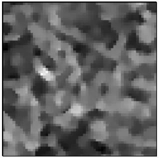

New reaction, $(X_{HP} - \hat{X}_{HP})^2$

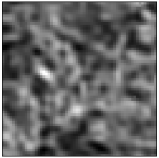

New tensor, $D(\nabla(X + \alpha Y_\phi))$

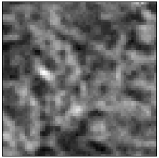

Modified PDE